HHS Public Access

Author manuscript

Free Radic Biol Med. Author manuscript; available in PMC 2019 February 20.

Published in final edited form as:

Free Radic Biol Med. 2018 February 20; 116: 134–140. doi:10.1016/j.freeradbiomed.2018.01.014.

Quantification of light-induced miniSOG superoxide production using the selective marker, 2-hydroxyethidium

Miriam E. Barnett[1], **Timothy M. Baran**[2], **Thomas H. Foster**[2], and **Andrew P. Wojtovich**[1,3,*]

[1]University of Rochester Medical Center, Department of Pharmacology and Physiology, Rochester, 14642, United States of America

[2]University of Rochester Medical Center, Department of Imaging Sciences, Rochester, 14642, United States of America

[3]University of Rochester Medical Center, Department of Anesthesiology and Perioperative Medicine, Rochester, 14642. United States of America

Abstract

Genetically-encoded photosensitizers produce reactive oxygen species (ROS) in response to light. Transgenic expression of fusion proteins can target the photosensitizers to specific cell regions and permit the spatial and temporal control of ROS production. These ROS-generating proteins (RGPs) are widely used for cell ablation, mutagenesis and chromophore-assisted light inactivation of target proteins. However, the species produced by RGPs are unclear due to indirect measures with confounding interpretations. Recently, the RGP mini "Singlet Oxygen Generator" (miniSOG) was engineered from *Arabidopsis thaliana* phototropin 2. While miniSOG produces singlet oxygen ($^1O_2$), the contribution of superoxide ($O_2^{\bullet-}$) to miniSOG-generated ROS remains unclear. We measured the light-dependent $O_2^{\bullet-}$ production of purified miniSOG using HPLC separation of dihydroethidium (DHE) oxidation products. We demonstrate that DHE is insensitive to $^1O_2$ and establish that DHE is a suitable indicator to measure $O_2^{\bullet-}$ production in a system that produces both $^1O_2$ and $O_2^{\bullet-}$. We report that miniSOG produces both $^1O_2$ and $O_2^{\bullet-}$, as can its free chromophore, flavin mononucleotide. miniSOG produced $O_2^{\bullet-}$ at a rate of ~4.0 μmol $O_2^{\bullet-}$/min/μmol photosensitizer for an excitation fluence rate of 5.9 mW/mm^2 at 470 ± 20 nm, and the rate remained consistent across fluences (light doses). Overall, the contribution of $O_2^{\bullet-}$ to miniSOG phenotypes should be considered.

Keywords

miniSOG; reactive oxygen species; singlet oxygen; superoxide; Flavin mononucleotide

*Corresponding author: Andrew_Wojtovich@urmc.rochester.edu.

Introduction

Photosensitizers produce reactive oxygen species (ROS) in response to light [1]. Reactive-oxygen-species-generating proteins, or RGPs, are a class of genetically-encoded photosensitizers [1]. These include SuperNova [2], KillerRed [3], KillerOrange [4], and miniSOG [5]. A RGP has the capability to generate different types of ROS including superoxide ($O_2^{\bullet-}$) and singlet oxygen ($^1O_2$). mini "Singlet Oxygen Generator" (miniSOG) is unique in that it generates a relatively large quantum yield of $^1O_2$ [5]. This ROS production is attributed to its chromophore flavin mononucleotide (FMN), a well-known $^1O_2$-generating photosensitizer [6, 7]. miniSOG has been used for a variety of applications, such as electron microscopy [5], cell death [8, 9], mutagenesis [10] and target protein inactivation [11, 12]. While miniSOG was successful for these applications, the ROS responsible remained unknown as the $^1O_2$ yield was debated [13, 14].

The disparity between $^1O_2$ yields with different detection methods led to the hypothesis that $O_2^{\bullet-}$ may be a species produced by miniSOG [13]. Pimenta *et al.* measured $O_2^{\bullet-}$ production using the fluorescence of dihydroethidium (DHE) oxidation products, a nonspecific measure of $O_2^{\bullet-}$. The fluorescence of DHE oxidation products can be the result of the $O_2^{\bullet-}$ specific product, 2-OHE$^+$, and the nonspecific product, E$^+$. These resulting DHE oxidation products are indistinguishable via fluorescence alone, and require HPLC separation to measure $O_2^{\bullet-}$ production specifically [15, 16]. Moreover, although based on fluorescence, there are conflicting results and no clear consensus on whether or not $^1O_2$ can react with DHE to form E$^+$ [17–19]. Overall, our goal was to clarify the impact of $^1O_2$ on DHE-oxidation products and confirm if miniSOG generates $O_2^{\bullet-}$ by measuring the formation of the $O_2^{\bullet-}$ specific DHE oxidation product, 2-OHE$^+$.

Thus, we measured $O_2^{\bullet-}$ generated by miniSOG using HPLC separation of the DHE oxidation products to specifically detect $O_2^{\bullet-}$. We characterized the measurement system using Rose Bengal, a chemical photosensitizer that generates both $O_2^{\bullet-}$ and $^1O_2$ [20–22]. Detailed DHE oxidation product analysis demonstrates that $^1O_2$ does not react with DHE. Under conditions where miniSOG makes $^1O_2$, it also produces $O_2^{\bullet-}$ at a flux that is consistent across fluences (light doses).

Materials and Methods

Singlet oxygen detection using singlet oxygen sensor green

$^1O_2$ was measured using singlet oxygen sensor green (SOSG; Molecular Probes). SOSG has a weak blue fluorescence but upon reaction with $^1O_2$ exhibits a strong green fluorescence [23]. SOSG (1μM) baseline fluorescence was measured in a cuvette containing a photosensitizer, Rose Bengal (RB, 2.5 μM; Sigma) or Deuteroporphyrin (DP, 2.5 μM; Frontier Scientific), and SOSG buffer (SB; 120 mM KCl, 25 mM sucrose, 5 mM $MgCl_2$, 5 mM KH_2PO_4, 1 mM EGTA, 10 mM HEPES, 0.1 mM DPTA, pH 7.3). Where indicated, 20 mM azide or 800 units/mL superoxide dismutase (SOD, Sigma) was present (as illustrated in scheme 1). Temperature was held constant at 25°C. The fluorescence (Ex 488 nm; Em 525 nm; slit width 5 nm) was recorded for 1 minute with constant stirring before and after illumination (560 ± 20 nm, 10.6 mW/mm^2) for 0–30 minutes. The change in fluorescence

intensity (post minus pre-illumination) was calculated. Experiments using FMN (10 μM) or purified miniSOG (10 μM) were illuminated at 470 ± 20 nm (5.9 mW/mm^2). To avoid spectral overlap with FMN, SOSG fluorescence was excited at 504 nm (Em 525 nm; slit width 5 nm). Structures of Rose Bengal and FMN are shown in Supplemental Fig. 1.

Light intensity was measured using a calibrated thermopile detector (818P-010-12, Newport Corporation, Irvine, CA) connected to an optical power meter (1916-R, Newport Corporation). For all experiments in which the illumination was varied, the intensity of light or fluence rate (watts/area) was held constant. The total fluence (joules/area) was altered by varying the illumination time.

Quantification of xanthine/xanthine oxidase superoxide production using cytochrome c

Xanthine oxidase (XO) catalyzes the oxidation of xanthine (X) to uric acid. During this reaction XO generates $O_2^{\bullet-}$ or H_2O_2 via either a 1 or 2 electron reduction, respectively. The rate of X/XO $O_2^{\bullet-}$ formation was measured as the rate of SOD-sensitive cytochrome *c* reduction. Briefly, at ambient O_2, XO (0.1 units/mL) and X (1 mM) were added to a 0.1 cm cuvette containing cytochrome *c* (800 mM). The rate of cytochrome *c* reduction was monitored at 550 nm and calculated using an extinction coefficient of 18.7 M^{-1} cm^{-1} in the presence or absence of SOD (800 units/mL) [24]. The X/XO reaction predominately generates H_2O_2 in a pH and oxygen concentration-dependent manner [25]. The percentage of $O_2^{\bullet-}$ generated by X/XO was calculated by dividing the $O_2^{\bullet-}$ generation by the total electron flux of X to uric acid by XO, as previously described by Kelley *et al.* [25].

Superoxide detection using HPLC separation of DHE oxidation products

Xanthine/xanthine oxidase (X/XO) system—$O_2^{\bullet-}$ was measured using dihydroethidium (DHE; Thermo Fisher Scientific) followed by HPLC separation of the resulting oxidation products [16]. Upon oxidation, DHE forms red fluorescent products, a $O_2^{\bullet-}$ specific product, 2-OHE$^+$, and a nonspecific product, E$^+$, which must be separated by HPLC due to overlapping fluorescence spectra [16, 26]. Structures of DHE, 2-OHE$^+$ and E$^+$ are shown in Supplemental Fig. 1. In 1 mL of PBS containing DPTA (DPBS; 7.78 mM Na_2HPO_4, 2.2 mM KH_2PO_4, 0.1 mM DPTA, pH 7.4 at 37°C) and DHE (50 μM), 0.1 units/mL XO and 1 mM X were added to generate $O_2^{\bullet-}$. Where indicated, 800 units/mL SOD was present (as illustrated in scheme 1). The solution was incubated at 37°C for 0–20 minutes (as indicated) to generate increasing amounts of $O_2^{\bullet-}$, after which the reaction was stopped with an equal volume of acidified methanol (200 mM $HClO_4$ in methanol). The solution was incubated at −20°C for 30 minutes and then centrifuged at 17,000 × *g*, 4°C for 20 minutes. Next, an equal volume of sample was combined with 1 M $K^+PO_4^-$ (pH 2.6). Again, the sample was incubated at −20°C for 30 minutes and then centrifuged at 17,000 × *g* for 10 minutes. Samples were separated on a Polar-RP column (Phenomenex, 150 × 2 mm; 4μm) run on Shimadzu HPLC with fluorescence detection (RF-20A). From 0 to 15 minutes the detector was on low sensitivity (channel 1: Ex: 358 nm, Em: 440 nm; channel 2: Ex: 490 nm, Em: 596 nm). After 15 minutes, the sensitivity switched to high (channel 1: Ex: 490 nm, Em: 567 nm; channel 2 remained constant) with a constant flow rate of 0.1 mL/min. Two mobile phases were used (A, 10% ACN with 0.1 %TFA in water; B, 60% ACN with 0.1 %TFA in water) using the following gradient: 0 min, 40% B; 5 min, 40% B; 25 min,

100% B; 30 min, 100% B; 35 min, 40% B; 40min, 40% B. Concentrations of DHE, 2-OHE^+ and E^+ were measured using standard curves. DHE and E^+ standards were commercially available. The 2-OHE^+ was made using X/XO generated $O_2^{\bullet -}$. The resulting mixture was separated using HPLC and the fraction containing 2-OHE^+ was collected and lyophilized to a dry powder. 2-OHE^+ was confirmed using mass spectrometry (URMC Mass Spectrometry Resource Laboratory; m/z = 330.16; the intervals between isotopic peaks = 1.0).

Photosensitizers—Superoxide production from photosensitizers was measured as described above with the following modifications. DHE (50 μM) and RB or DP (2.5 μM) were illuminated (560 ± 20 nm, 17 mW/mm^2) in assay buffer (120 mM KCl, 25 mM sucrose, 5 mM $MgCl_2$, 5 mM KH_2PO_4, 1 mM EGTA, 10 mM HEPES, 0.1 mM DPTA, pH 7.3) for 0–5 minutes. As a control, one cuvette was also incubated in the dark. Where indicated, 20 mM azide or 800 units/mL SOD or 4,200 units/mL of catalase (CAT, 1 mg/mL; from bovine liver or from Corynebacterium glutamicum as indicated, Sigma) or hydrogen peroxide (H_2O_2, Sigma) was present. The procedure was repeated with 10 μM free FMN (Sigma) or purified miniSOG. Samples were illuminated at 470 ± 20 nm (5.9 mW/mm^2).

miniSOG Purification

Recombinant miniSOG with an N-terminal histidine tag was expressed and purified from BL21DE3pLYS cells. Briefly, the coding region of miniSOG (courtesy of Drs. Roger Tsien and Yishi Jin, University of California, San Diego) was inserted in pRSET B using BamHI and EcoRI. The plasmid was electroporated into competent BL21pLyS cells and plated on ampicillin plates (100 μg/mL). A single colony was grown to OD_{600} of 0.5 and miniSOG expression was induced using IPTG (100 μM). Cells were grown in the dark and lysed after 4 hours of expression with lysis buffer (3% SDS, 50 mM Tris, pH 8.0) and protease inhibitors (Pierce). His-tagged miniSOG was then allowed to bind to Ni-NTA agarose beads (Qiagen) overnight; fluorescence was monitored to ensure protein binding. miniSOG was eluted with 100 μM imidazole and desalted with a PD-10 column (GE Healthcare). The sample was concentrated using a centrifugal filter with a 10 KDa cutoff (Amicon) and stored in 10% glycerol PBS buffer, at 4°C. To ensure that miniSOG ROS generation was only due to miniSOG bound FMN, ROS measurements were taken immediately after concentrating, thus ensuring any free FMN would be removed. The entire purification process was performed in the dark and the protein was protected from light. The resulting protein was characterized by measuring the extinction coefficient, fluorescent quantum yield using fluorescein as standard (ΦF = 0.95) [27], and the absorption and emission spectra. Since the purified miniSOG contained both mature (FMN-containing) and immature (void of FMN) protein, the concentration of mature functional protein was determined using the extinction coefficient of flavin as previously described [13]. Briefly, miniSOG was denatured to release FMN and the concentration of free FMN (ε=12,500 ± 500 M^{-1} cm^{-1} at 450 nm) [28, 29] was determined using a standard curve. Since a mature photoactivatable miniSOG contains a single FMN as its chromophore, the concentration of FMN was assumed to equal the concentration of mature miniSOG [5, 13, 14].

Results

Detection of $O_2^{\bullet-}$ using HPLC separated DHE-oxidation products

First, we characterized the HPLC separation and fluorescent detection of DHE oxidation products using the X/XO generated $O_2^{\bullet-}$ (Fig. 1). Importantly, the X/XO reaction does not generate $^1O_2$ and moreover, a reaction product, uric acid, is an efficient $^1O_2$ scavenger [30]. Thus, we attribute changes in DHE oxidation products to $O_2^{\bullet-}$ and resulting dismutation products. We observed an incubation-time-dependent increase in 2-OHE$^+$ (Fig 1A) with a minimal impact on the E$^+$ component. SOD, which scavenges $O_2^{\bullet-}$ 1,000 times faster than it can react with the DHE [16], significantly decreased the amount of detectable 2-OHE$^+$, while the E$^+$ component was unaffected (Fig. 1B). We attempted to mimic the inhibitory effect of SOD on 2-OHE$^+$ formation using the chemical $O_2^{\bullet-}$ scavenger, TEMPO, but found that TEMPO converted all of the DHE to E$^+$, thereby preventing any possible 2-OHE$^+$ formation (Supplemental Fig. 2). This is consistent with a previous result, which observed an increased fluorescence in DHE products in the presence of TEMPOL [31]. Our findings confirm the E$^+$, not 2-OHE$^+$, contribution to the observed fluorescence signal [19]. We conclude that the HPLC separation of DHE oxidation products can measure $O_2^{\bullet-}$ production via 2-OHE$^+$ formation in an SOD-sensitive manner.

We sought to quantify the superoxide production rate of miniSOG, however, the ratio of 2-OHE$^+$ formation to $O_2^{\bullet-}$ is not linear. Given a fourfold difference in X/XO incubation time (5 min vs. 20 min), the 2-OHE$^+$ concentration only doubled (Fig. 1B). A recent report demonstrated that the stoichiometry of $O_2^{\bullet-}$ molecules to 2-OHE$^+$ formation varies with the concentration of $O_2^{\bullet-}$ [15]. For low concentrations of $O_2^{\bullet-}$, the $O_2^{\bullet-}$ to 2-OHE$^+$ ratio is 2:1 and increases nonlinearly with the concentration of $O_2^{\bullet-}$ [15]. The increase in the $O_2^{\bullet-}$:2-OHE$^+$ ratio is hypothesized to be the result of increased $O_2^{\bullet-}$ dismutation [15]. Therefore, in order to equate 2-OHE$^+$ formation with $O_2^{\bullet-}$, we first determined the $O_2^{\bullet-}$ production capabilities of X/XO using cytochrome *c* reduction. Secondly, we incubated X/XO with DHE for various incubation times and measured 2-OHE$^+$.

XO produces both H_2O_2 and $O_2^{\bullet-}$ in a pH and oxygen dependent manner [25]. The rate of $O_2^{\bullet-}$ production was measured via cytochrome *c* reduction. Under conditions that mimic DHE experiments, the $O_2^{\bullet-}$ flux of X/XO was 60.5 ± 8.7 μM/min. This rate demonstrates that 30.3% of total XO electron flux results in $O_2^{\bullet-}$ and is consistent with a previous report [25]. Next, we measured 2-OHE$^+$ formation as a function of time to mimic photosensitizer $O_2^{\bullet-}$ formation (Fig. 1C). The cumulative amount of 2-OHE$^+$ generated during a period was plotted as a function of cumulative $O_2^{\bullet-}$ generated. The stoichiometry of $O_2^{\bullet-}$ to 2-OHE$^+$ is in agreement with previous reports [15] and follows a logarithmic relationship. Using X/XO $O_2^{\bullet-}$ generation as a standard, we can quantify $O_2^{\bullet-}$ production using 2-OHE$^+$ formation.

Next, to determine whether DHE is suitable for measuring photosensitizer-generated ROS, we measured DHE oxidation products resulting from the illumination of Rose Bengal (RB). Since RB is known to generate large quantities of $^1O_2$ and to a lesser amount $O_2^{\bullet-}$ [6, 7, 22], it served as a control to determine if $^1O_2$ has confounding effects on the DHE oxidation products. Additionally, DHE is light-sensitive and can undergo photo-oxidation [32]. The illumination of Singlet Oxygen Sensor Green (SOSG) or DHE alone did not prevent the

detection of photosensitizer-generated $^1O_2$ or $O_2^{\bullet-}$ (see figure legends for each wavelength). When RB was illuminated, $^1O_2$ was detected (Fig. 2 A) and we found the rapid formation of DHE-oxidation products (Fig. 2B). Notably, both the 2-OHE$^+$ and E$^+$ components were insensitive to the $^1O_2$ scavenger azide (Fig. 2C, p = 0.16; p = 0.13; 5 min light vs 5 min light + azide for 2-OHE$^+$ and E$^+$, respectively), which suggests that DHE is insensitive to $^1O_2$. Consistent with the X/XO data, SOD specifically reduced RB generated 2-OHE$^+$, suggesting we can detect $O_2^{\bullet-}$ despite the presence of $^1O_2$. Similar results were found using another chemical photosensitizer, deuteroporphyrin (DP, Supplemental Fig. 3). Collectively, these results demonstrate that the formation of the $O_2^{\bullet-}$-selective DHE oxidation product 2-OHE$^+$ is SOD-sensitive and that azidesensitive $^1O_2$ does not impact its formation, as seen in scheme 1.

miniSOG $^1O_2$ generation

Given that the HPLC separation of DHE oxidation products can measure $O_2^{\bullet-}$ in the presence of $^1O_2$, we next sought to determine if miniSOG produces $O_2^{\bullet-}$. We purified miniSOG and the resulting protein had an extinction coefficient of $15.15 \pm 0.9 \times 10^3$ M^{-1} cm^{-1}, fluorescence quantum yield of 0.35 ± 0.017, and an expected molecular weight (Supplemental Fig. 4) as previously reported [5, 13]. miniSOG is a small protein that encapsulates a flavin mononucleotide (FMN), which acts as the photosensitizer. In order to understand its ROS production, we therefore compared miniSOG to its free chromophore, FMN. Both FMN and miniSOG generate $^1O_2$ in response to light [5]. We first determined if miniSOG was functional by detecting $^1O_2$ via Singlet Oxygen Sensor Green (SOSG).

We found that both FMN and miniSOG behaved similarly, with SOSG fluorescence steadily increasing with illumination time until a peak value was reached (Fig. 3A, C). Notably, FMN produced a larger amount of detectable $^1O_2$ at a faster rate than miniSOG (99.5 a.u./min versus 24.6 a.u./min, FMN vs. miniSOG, respectively). This supports the lower published $^1O_2$ quantum yield of miniSOG [13, 14]. However, both reached asymptotic levels following prolonged irradiation (Fig. 3A, C). Azide prevented the FMN- and miniSOG-mediated SOSG fluorescence increase, suggesting a $^1O_2$-dependent mechanism (Fig. 3B, D). As expected, fluorescence was not lost with SOD (Fig. 3B, D). These results demonstrate that the purified miniSOG is functional and, like FMN, can generate $^1O_2$.

miniSOG $O_2^{\bullet-}$ generation

Similar to RB, FMN generates both $^1O_2$ (Fig. 3) and $O_2^{\bullet-}$ in response to light [6, 7]. However, the precise mechanism of light-induced miniSOG ROS production was unclear. We hypothesized that miniSOG could produce both $^1O_2$ and $O_2^{\bullet-}$ in a manner similar to its free photosensitizer, FMN. Alternatively, miniSOG's protein encapsulation of the FMN could alter its ROS production properties to favor a particular photosensitization mechanism. Thus, we next measured the $O_2^{\bullet-}$ production of FMN and miniSOG using HPLC separation of DHE oxidation products, as seen in scheme 1. FMN and miniSOG were incubated with DHE and illuminated for various amounts of time (Fig. 4A, C). Both FMN and miniSOG produced 2-OHE$^+$, but miniSOG did so to a lesser extent. SOD significantly reduced the 2-OHE$^+$ components in both systems ($p < 0.001$, Fig. 4B, D). While azide had no effect on miniSOG-mediated 2-OHE$^+$ formation (p=0.22, 5 min light vs 5 min light + azide, Fig. 4D),

azide significantly reduced the 2-OHE$^+$ component in the FMN system (Fig. 4B). We hypothesize that the reduction is due to azide directly interacting with the excited state of FMN [33] rather than scavenging ROS. Light excites FMN to its triplet state, which can then interact with O_2 to form either $O_2^{\bullet-}$ or $^1O_2$. Azide can prevent the generation of ROS by interacting with FMN's excited state, thus preventing FMN's ability to react with O_2 [33]. Azide quenches $^1O_2$ with $K_Q \sim 2$ to 4×10^8 $M^{-1}s^{-1}$; however, azide additionally quenches the triplet state of FMN at a rate of ~ 2 to 5×10^9 $M^{-1}s^{-1}$ [7]. Thus, the decrease in FMN light-dependent 2-OHE$^+$ formation in the presence of azide may be the result of azide preventing ROS formation rather than scavenging it (Fig. 4B). In support of this hypothesis, uric acid, a different $^1O_2$ scavenger significantly decreased FMN $^1O_2$ production with no effect on $O_2^{\bullet-}$ generation (Supplemental Fig. 5). Azide did not have the same impact on 2-OHE$^+$ generation for miniSOG as it did with free FMN (Fig. 4D).

In order to quantify miniSOG $O_2^{\bullet-}$ rates, we used the ratio of $O_2^{\bullet-}$:2-OHE$^+$ calculated from the X/XO system (Fig. 1C). A previous report had demonstrated that miniSOG's $^1O_2$ quantum yield is light dose-dependent [14]. Thus, we determined the $O_2^{\bullet-}$ flux-dependence on light dose (Supplemental Fig. 6). miniSOG's $O_2^{\bullet-}$ remained constant at ~4.0 μmol $O_2^{\bullet-}$/min/μmol photosensitizer for an excitation fluence rate of 5.9 mW/mm^2 at 470 ± 20 nm and was independent of light dose (Supplemental Fig. 6).

A previous study utilized catalase-sensitive DHE fluorescence to elude to miniSOG-mediated $O_2^{\bullet-}$ formation [13]. Catalase decomposes hydrogen peroxide (H_2O_2) to water and oxygen and has no direct effect on $O_2^{\bullet-}$. Moreover, H_2O_2 does not directly react with DHE [19]. Thus, we examined the impact of H_2O_2 and catalase on DHE oxidation products. We found that H_2O_2 increased E$^+$ formation in a catalase-dependent manner and the addition of catalase alone increased E$^+$ formation through an unknown mechanism (Supplemental Fig. 7). Impurities in the H_2O_2 solution or the catalase preparation may contribute the increased E$^+$ formation. However, catalase from *Corynebacterium glutamicum* yielded a finding similar to catalase from bovine liver (DHE alone, 112 ± 30 pmol/mL 2-OHE$^+$ and 1583 ± 423 pmol/mL E$^+$; DHE plus *C. glutamicum* catalase, 317 ± 31 pmol/mL 2-OHE$^+$ and 7405 ± 1397 pmol/mL E$^+$). Despite the impact of catalase on E$^+$ generation (Supplemental Fig. 7), we sought to confirm if catalase could decrease miniSOG generated 2-OHE$^+$ formation [13]. The addition of catalase to the FMN or miniSOG photosensitization reaction had no effect on the 2-OHE$^+$ component (Fig. 5B, C) and is contrary to a previous report [13]. We suggest that the difference can be attributed to analyzing fluorescence alone as opposed to in combination with HPLC separation.

Discussion

Genetically-encoded photosensitizers contain a chromophore, which when illuminated can generate ROS. The miniSOG chromophore, FMN, is relatively well-studied, has a $^1O_2$ quantum yield of 0.51 and generates $O_2^{\bullet-}$ [5, 34]. However, by encapsulating this chromophore, miniSOG's ROS-producing capabilities may be altered. miniSOG's $^1O_2$-generating capabilities are reported elsewhere [5, 13, 14]; however, it was unclear if it could produce $O_2^{\bullet-}$, since previous studies relied on indirect measures of $O_2^{\bullet-}$ and used catalase as a scavenger [13].

While DHE is a commonly used $O_2^{\bullet-}$ detector, fluorescence alone does not indicate the presence of $O_2^{\bullet-}$ due to the formation of a nonspecific oxidation product [15, 16]. Additionally, catalase, an enzyme that removes H_2O_2 from the system, should not impact $O_2^{\bullet-}$ (scheme 1). Lastly, it was unknown whether or not $^1O_2$ could impact the oxidation of DHE [17–19]. Consequently, a report that miniSOG generates $O_2^{\bullet-}$ based on catalase-sensitive fluorescence spectra was inconclusive [13]. We improve upon these measurements by isolating the $O_2^{\bullet-}$-specific product by HPLC separation. The data presented herein demonstrate that despite the presence of both $^1O_2$ and $O_2^{\bullet-}$, we found no evidence that $^1O_2$ impacted the $O_2^{\bullet-}$-selective DHE oxidation product (Fig. 2C). We demonstrate that miniSOG generates $O_2^{\bullet-}$ in an SOD-dependent and azide/catalase-independent manner. miniSOG's $O_2^{\bullet-}$ production rate was lower than its free chromophore and insensitive to light dose. Interestingly, while azide directly interacted with the excited state of FMN to prevent ROS formation, azide did not have the same effect on miniSOG. This is consistent with a lack of access to FMN in the protein or a shift in the triplet state energy of bound FMN, rendering the quenching by azide less efficient. Together, these data demonstrate that the surrounding protein can influence ROS flux from miniSOG.

The $^1O_2$ quantum yield of miniSOG is lower than that of FMN [13, 14]. One of the contributing factors to the difference in yield is miniSOG's protein encapsulation of FMN. Ruiz-Gonzalez *et al.* monitored the time-resolved phosphorescence of miniSOG-generated $^1O_2$ with increasing fluence (0–400 J/cm^2) and found a ~10-fold increase in $^1O_2$ quantum yield [14]. The authors hypothesize that this increase in yield is due to inactivation of $^1O_2$ quenching amino acid residues in miniSOG [14]. Thus, the $^1O_2$ quantum yield of miniSOG ranges from 0.03 to ~0.30 and is directly related to fluence [13, 14]. In contrast to $^1O_2$, we found no change in the $O_2^{\bullet-}$ production rate with increasing light dose (0–177 J/cm^2, Supplemental Fig. 6), suggesting that $O_2^{\bullet-}$ is able to freely diffuse out of the protein.

Each ROS has unique chemical properties, which may permit preference towards a biological target [35, 36]. For example, $O_2^{\bullet-}$ has a high reaction rate with iron-sulfur clusters, while $^1O_2$ by comparison has a more indiscriminate reactivity [35, 36]. miniSOG is used in various applications ranging from electron microscopy to photoablation [5, 8–12]. Understanding the type and amount of biologically available ROS produced by miniSOG can improve the experimental design and interpretation of the results.

Conclusion

Genetically-encoded photosensitizers that produce ROS are important tools for redox biology. Proteins such as miniSOG, offer spatial and temporal control over ROS production [1]. However, a complete study of their ROS-generating capability is limited and hampers further development of the optogenetic toolbox. Our results demonstrate that, in addition to $^1O_2$, miniSOG generates $O_2^{\bullet-}$ in response to light, much like its FMN chromophore. The $O_2^{\bullet-}$ production rate was determined using HPLC separation and fluorescence detection of the $O_2^{\bullet-}$-selective product, 2-OHE$^+$. These results addressed the confounding interpretations using nonspecific readouts of fluorescence alone. The contribution of each ROS to the overall output of miniSOG is light dose-dependent and should be considered in future studies.

Supplementary Material

Refer to Web version on PubMed Central for supplementary material.

Acknowledgments

We thank Paul Brookes and members of the University of Rochester Medical Center's Mitochondrial Research Group for helpful discussions. This work was supported by the National Institutes of Health to APW (R01 NS092558) and an Institutional Ruth L. Kirschstein National Research Service Award (GM068411) to MB.

References

1. Wojtovich AP, Foster TH. Optogenetic control of ROS production. Redox Biol. 2014; 2:368–76. [PubMed: 24563855]
2. Takemoto K, Matsuda T, Sakai N, Fu D, Noda M, Uchiyama S, Kotera I, Arai Y, Horiuchi M, Fukui K, Ayabe T, Inagaki F, Suzuki H, Nagai T. SuperNova, a monomeric photosensitizing fluorescent protein for chromophore-assisted light inactivation. Sci Rep. 2013; 3:2629. [PubMed: 24043132]
3. Bulina ME, Chudakov DM, Britanova OV, Yanushevich YG, Staroverov DB, Chepurnykh TV, Merzlyak EM, Shkrob MA, Lukyanov S, Lukyanov KA. A genetically encoded photosensitizer. Nat Biotechnol. 2006; 24(1):95–9. [PubMed: 16369538]
4. Sarkisyan KS, Zlobovskaya OA, Gorbachev DA, Bozhanova NG, Sharonov GV, Staroverov DB, Egorov ES, Ryabova AV, Solntsev KM, Mishin AS, Lukyanov KA. KillerOrange, a Genetically Encoded Photosensitizer Activated by Blue and Green Light. Plos One. 2015; 10(12)
5. Shu X, Lev-Ram V, Deerinck TJ, Qi Y, Ramko EB, Davidson MW, Jin Y, Ellisman MH, Tsien RY. A genetically encoded tag for correlated light and electron microscopy of intact cells, tissues, and organisms. PLoS Biol. 2011; 9(4):e1001041. [PubMed: 21483721]
6. Silva E, Edwards AM, Pacheco D. Visible light-induced photooxidation of glucose sensitized by riboflavin. J Nutr Biochem. 1999; 10(3):181–5. [PubMed: 15539287]
7. Spikes JD, Shen HR, Kopeckova P, Kopecek J. Photodynamic crosslinking of proteins. III. Kinetics of the FMN- and rose bengal-sensitized photooxidation and intermolecular crosslinking of model tyrosine-containing N-(2-hydroxypropyl)methacrylamide copolymers. Photochem Photobiol. 1999; 70(2):130–7. [PubMed: 10461454]
8. Qi YB, Garren EJ, Shu X, Tsien RY, Jin Y. Photo-inducible cell ablation in Caenorhabditis elegans using the genetically encoded singlet oxygen generating protein miniSOG. Proc Natl Acad Sci U S A. 2012; 109(19):7499–504. [PubMed: 22532663]
9. Xu S, Chisholm AD. Highly efficient optogenetic cell ablation in C. elegans using membrane-targeted miniSOG. Sci Rep. 2016; 6:21271. [PubMed: 26861262]
10. Noma K, Jin Y. Optogenetic mutagenesis in Caenorhabditis elegans. Nat Commun. 2015; 6:8868. [PubMed: 26632265]
11. Wojtovich AP, Wei AY, Sherman TA, Foster TH, Nehrke K. Chromophore-Assisted Light Inactivation of Mitochondrial Electron Transport Chain Complex II in Caenorhabditis elegans. Sci Rep. 2016; 6:29695. [PubMed: 27440050]
12. Makhijani K, To TL, Ruiz-Gonzalez R, Lafaye C, Royant A, Shu X. Precision Optogenetic Tool for Selective Single- and Multiple-Cell Ablation in a Live Animal Model System. Cell Chem Biol. 2017; 24(1):110–119. [PubMed: 28065655]
13. Pimenta FM, Jensen RL, Breitenbach T, Etzerodt M, Ogilby PR. Oxygen-dependent photochemistry and photophysics of "miniSOG," a protein-encased flavin. Photochem Photobiol. 2013; 89(5):1116–26. [PubMed: 23869989]
14. Ruiz-Gonzalez R, Cortajarena AL, Mejias SH, Agut M, Nonell S, Flors C. Singlet oxygen generation by the genetically encoded tag miniSOG. J Am Chem Soc. 2013; 135(26):9564–7. [PubMed: 23781844]
15. Michalski R, Michalowski B, Sikora A, Zielonka J, Kalyanaraman B. On the use of fluorescence lifetime imaging and dihydroethidium to detect superoxide in intact animals and ex vivo tissues: a reassessment. Free Radic Biol Med. 2014; 67:278–84. [PubMed: 24200598]

16. Zielonka J, Vasquez-Vivar J, Kalyanaraman B. Detection of 2-hydroxyethidium in cellular systems: a unique marker product of superoxide and hydroethidine. Nat Protoc. 2008; 3(1):8–21. [PubMed: 18193017]
17. Bilski PJ, Karriker B, Chignell CF. Quenching and generation of singlet oxygen by hydroethidine and related chromophores. Chemical Physics Letters. 2009; 475(1–3):116–119.
18. Bindokas VP, Jordan J, Lee CC, Miller RJ. Superoxide production in rat hippocampal neurons: selective imaging with hydroethidine. J Neurosci. 1996; 16(4):1324–36. [PubMed: 8778284]
19. Zielonka J, Kalyanaraman B. Hydroethidine- and MitoSOX-derived red fluorescence is not a reliable indicator of intracellular superoxide formation: another inconvenient truth. Free Radic Biol Med. 2010; 48(8):983–1001. [PubMed: 20116425]
20. Gottschalk P, Paczkowski J, Neckers DC. Factors Influencing the Quantum Yields for Rose-Bengal Formation of Singlet Oxygen. Journal of Photochemistry. 1986; 35(3):277–281.
21. Lamberts JJM, Neckers DC. Rose-Bengal Derivatives as Singlet Oxygen Sensitizers. Tetrahedron. 1985; 41(11):2183–2190.
22. Lee PC, Rodgers MA. Laser flash photokinetic studies of rose bengal sensitized photodynamic interactions of nucleotides and DNA. Photochem Photobiol. 1987; 45(1):79–86. [PubMed: 3031708]
23. Gollmer A, Arnbjerg J, Blaikie FH, Pedersen BW, Breitenbach T, Daasbjerg K, Glasius M, Ogilby PR. Singlet Oxygen Sensor Green(R): photochemical behavior in solution and in a mammalian cell. Photochem Photobiol. 2011; 87(3):671–9. [PubMed: 21272007]
24. Margoliash E, Frohwirt N. Spectrum of horse-heart cytochrome c. Biochem J. 1959; 71(3):570–2. [PubMed: 13638266]
25. Kelley EE, Khoo NK, Hundley NJ, Malik UZ, Freeman BA, Tarpey MM. Hydrogen peroxide is the major oxidant product of xanthine oxidase. Free Radic Biol Med. 2010; 48(4):493–8. [PubMed: 19941951]
26. Zhao H, Joseph J, Fales HM, Sokoloski EA, Levine RL, Vasquez-Vivar J, Kalyanaraman B. Detection and characterization of the product of hydroethidine and intracellular superoxide by HPLC and limitations of fluorescence. Proc Natl Acad Sci U S A. 2005; 102(16):5727–32. [PubMed: 15824309]
27. Magde D, Wong R, Seybold PG. Fluorescence quantum yields and their relation to lifetimes of rhodamine 6G and fluorescein in nine solvents: improved absolute standards for quantum yields. Photochem Photobiol. 2002; 75(4):327–34. [PubMed: 12003120]
28. Drepper T, Eggert T, Circolone F, Heck A, Krauss U, Guterl JK, Wendorff M, Losi A, Gartner W, Jaeger KE. Reporter proteins for in vivo fluorescence without oxygen. Nat Biotechnol. 2007; 25(4):443–5. [PubMed: 17351616]
29. Mukherjee A, Walker J, Weyant KB, Schroeder CM. Characterization of flavin-based fluorescent proteins: an emerging class of fluorescent reporters. PLoS One. 2013; 8(5):e64753. [PubMed: 23741385]
30. Sueishi Y, Hori M, Ishikawa M, Matsu-Ura K, Kamogawa E, Honda Y, Kita M, Ohara K. Scavenging rate constants of hydrophilic antioxidants against multiple reactive oxygen species. J Clin Biochem Nutr. 2014; 54(2):67–74. [PubMed: 24688213]
31. Burnaugh L, Sabeur K, Ball BA. Generation of superoxide anion by equine spermatozoa as detected by dihydroethidium. Theriogenology. 2007; 67(3):580–9. [PubMed: 17045638]
32. Zielonka J, Vasquez-Vivar J, Kalyanaraman B. The confounding effects of light, sonication, and Mn(III)TBAP on quantitation of superoxide using hydroethidine. Free Radic Biol Med. 2006; 41(7):1050–7. [PubMed: 16962930]
33. Heelis PF. The Photophysical and Photochemical Properties of Flavins (Isoalloxazines). Chem Soc Rev. 1982; 11(1):15–39.
34. Redmond RW, Gamlin JN. A compilation of singlet oxygen yields from biologically relevant molecules. Photochem Photobiol. 1999; 70(4):391–475. [PubMed: 10546544]
35. Bachi A, Dalle-Donne I, Scaloni A. Redox proteomics: chemical principles, methodological approaches and biological/biomedical promises. Chem Rev. 2013; 113(1):596–698. [PubMed: 23181411]

36. D'Autreaux B, Toledano MB. ROS as signalling molecules: mechanisms that generate specificity in ROS homeostasis. Nat Rev Mol Cell Biol. 2007; 8(10):813–24. [PubMed: 17848967]

Highlights

- Oxidation of dihydroethidium establishes miniSOG-mediated $O_2^{\bullet -}$ generation
- HPLC separation of $O_2^{\bullet -}$-selective marker, 2-hydroethidium quantified miniSOG $O_2^{\bullet -}$
- miniSOG $O_2^{\bullet -}$ production rate was consistent over a range of fluences

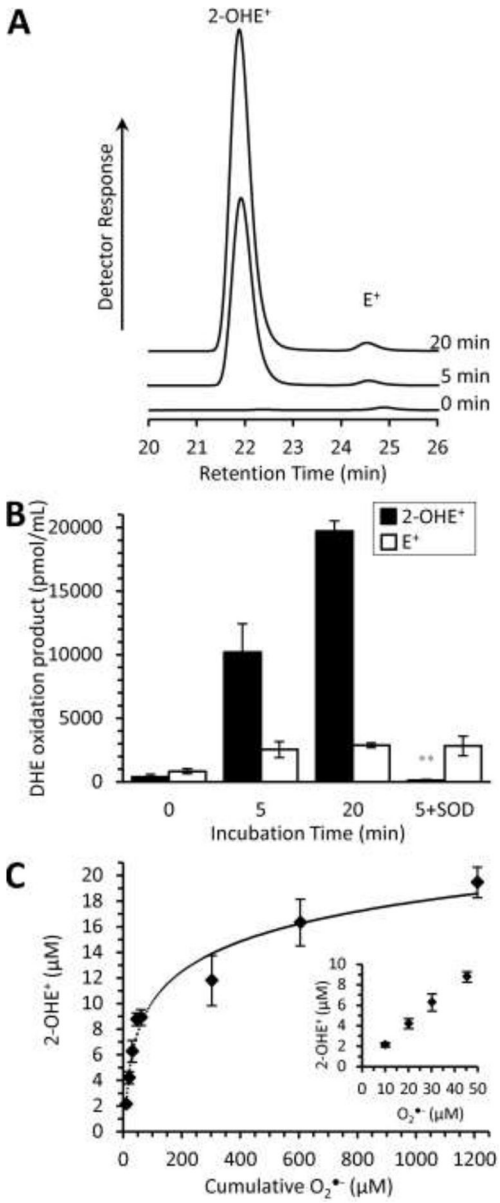

Fig. 1.

Characterization of DHE oxidation products derived from xanthine/xanthine oxidase generated ROS. (A) Representative HPLC traces of the fluorescence versus retention time separation of xanthine/xanthine oxidase generated 2-OHE$^+$ and E$^+$. Xanthine (X, 1mM) and xanthine oxidase (XO, 0.1 units/mL) were incubated for increasing amounts of time to generate $O_2^{\bullet-}$ in the presence of DHE (50 μM). The resulting DHE oxidation products were separated via HPLC. Using fluorescence detection, peaks at 22.0 and 24.5 minutes correspond to 2-OHE$^+$ and E$^+$, respectively. DHE was not limiting. (B) Peaks were integrated and quantified using a standard curve. The addition of SOD (800 U/mL) to X/XO reduced the 2-OHE$^+$ component while not effecting E$^+$. (C) 2-OHE$^+$ formation is dependent on the concentration of $O_2^{\bullet-}$. Using the cytochrome *c* reduction assay, X/XO $O_2^{\bullet-}$ production was determined to be 60.5 ± 8.7 μM/min. XO and X were incubated for

increasing amounts of time in the presence of DHE as in A, B to generate 2-OHE^+ as a function of time. The ratio of $O_2^{\bullet-}$ to 2-OHE^+ was found to be logarithmic (y=3.3838ln(x)–5.4326; R^2 = 0.97). Inset is 2-OHE^+ formation at the lower $O_2^{\bullet-}$ concentrations. All data are means ± SEM, N > 4. ** $p < 0.01$ versus 5-minute incubation (2-way ANOVA with Tukey correction).

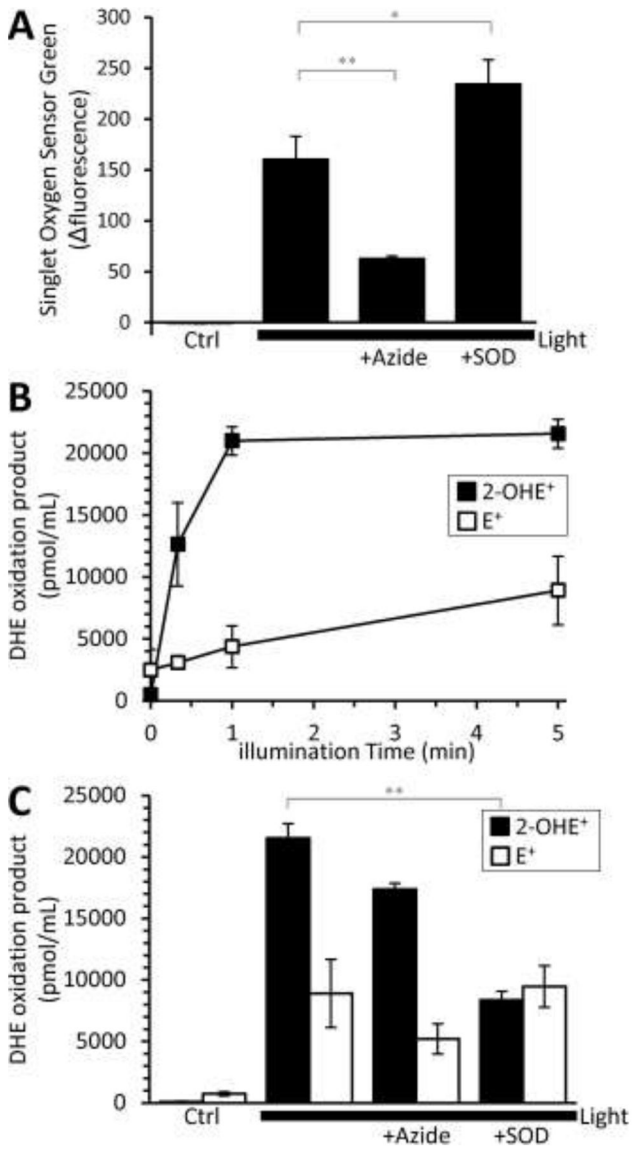

Fig. 2.

Detection of Rose Bengal (RB) $O_2^{\bullet-}$ production by DHE. (A) RB was illuminated (560 ± 20 nm, 10.6 mW/mm^2) for 5 minutes in the presence of Singlet Oxygen Sensor Green (SOSG). $^1O_2$ production was determined by the change in SOSG fluorescence intensity. The $^1O_2$ scavenger, azide (20 mM) or $O_2^{\bullet-}$ scavenger superoxide dismutase (SOD, 800 U/mL) was present where indicated. Azide or SOD in the presence of SOSG in the dark alone had no effect. SOSG illuminated for 5 minutes in the absence of photosensitizer yielded a change in fluorescence of −6.28 ± 1.4 a.u. Since RB has a large $^1O_2$ quantum yield, we wanted to determine if we were still able to detect $O_2^{\bullet-}$ with dihydroethidium (DHE). (B, C) RB (2.5 μM) was illuminated under the same conditions for increasing amounts of time in the presence of DHE (50 μM). Peaks, 2-OHE$^+$ and E$^+$, were integrated and quantified using a standard curve. The formation of the $O_2^{\bullet-}$ specific product, 2-OHE$^+$, is sensitive to SOD, as the addition of SOD (800 U/mL) reduced the 2-OHE$^+$ component while not effecting the E$^+$

component. Azide (20 mM) had no effect on either component, 2-OHE^+ or E^+. DHE illuminated for 5 minutes resulted in 258 ± 186 pmol/mL 2-OHE^+ and 607 ± 423 pmol/mL E^+. All data are means ± SEM, N > 4. ** $p < 0.01$ versus 5-minute light (2-way ANOVA with Tukey correction).

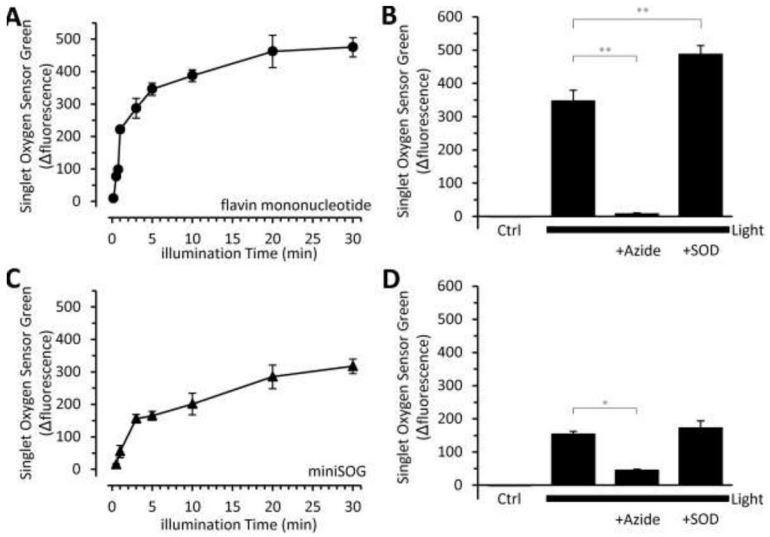

Fig. 3.

Singlet oxygen sensor green (SOSG) detection of flavin mononucleotide (FMN) and miniSOG generated $^1O_2$. (A) Free flavin mononucleotide (FMN) and (C) purified miniSOG were illuminated (470 ± 20 nm; 5.9 mW/mm^2) for the indicated time in the presence of SOSG. $^1O_2$ production was determined by the change in SOSG fluorescence intensity. Note: SOSG was excited at 504 nm. Where indicated, the $^1O_2$ scavenger, azide (20 mM) or $O_2^{\bullet -}$ scavenger, SOD (800 U/mL) were present when (B) free FMN or (D) miniSOG were illuminated for 5 minutes. SOSG illuminated for 5 minutes yielded a change in fluorescence of −1.53 ± 0.3 a.u. All data are means ± SEM, N > 4. *p<0.05, **p<0.01 versus 5-minute light (2-way ANOVA with Tukey correction).

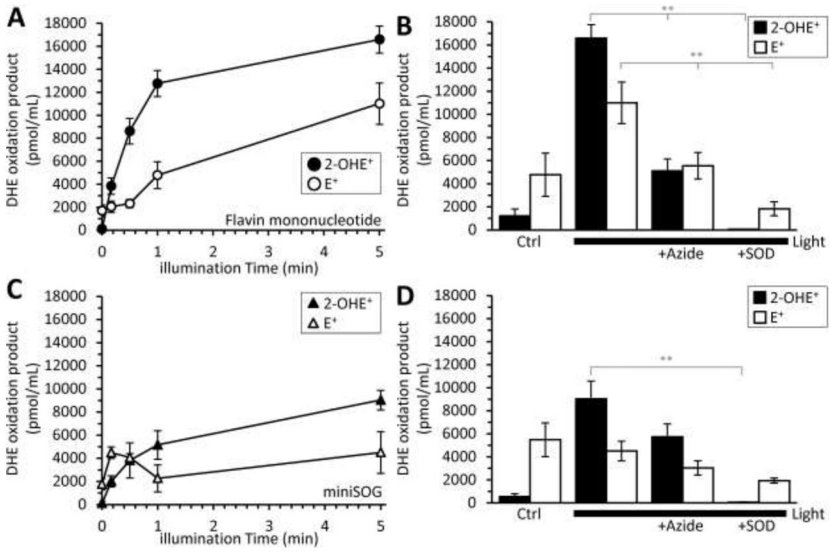

Fig. 4.

Detection of FMN and miniSOG light-dependent $O_2^{\bullet-}$ generation using HPLC separation of DHE oxidation products. (A) free FMN (10 μM) or (C) purified miniSOG (10 μM) were illuminated (470 ± 20 nm; 5.9 mW/mm^2) for increasing amounts of time in the presence of DHE (50 μM). The resulting 2-OHE$^+$ or E$^+$ peaks were integrated and quantified using a standard curve. Where indicated, the $^1O_2$ scavenger, azide (20 mM), $O_2^{\bullet-}$ scavenger, SOD (800 U/mL) were present when (B) free FMN or (D) miniSOG were illuminated for 5 minutes. DHE illuminated for 5 minutes resulted in 50 ± 17 pmol/mL 2-OHE$^+$ and 673 ± 142 pmol/mL E$^+$. All data are means ± SEM, N > 4. *p<0.05, ** p <0.01 versus 5-minute light (2-way ANOVA with Tukey correction.

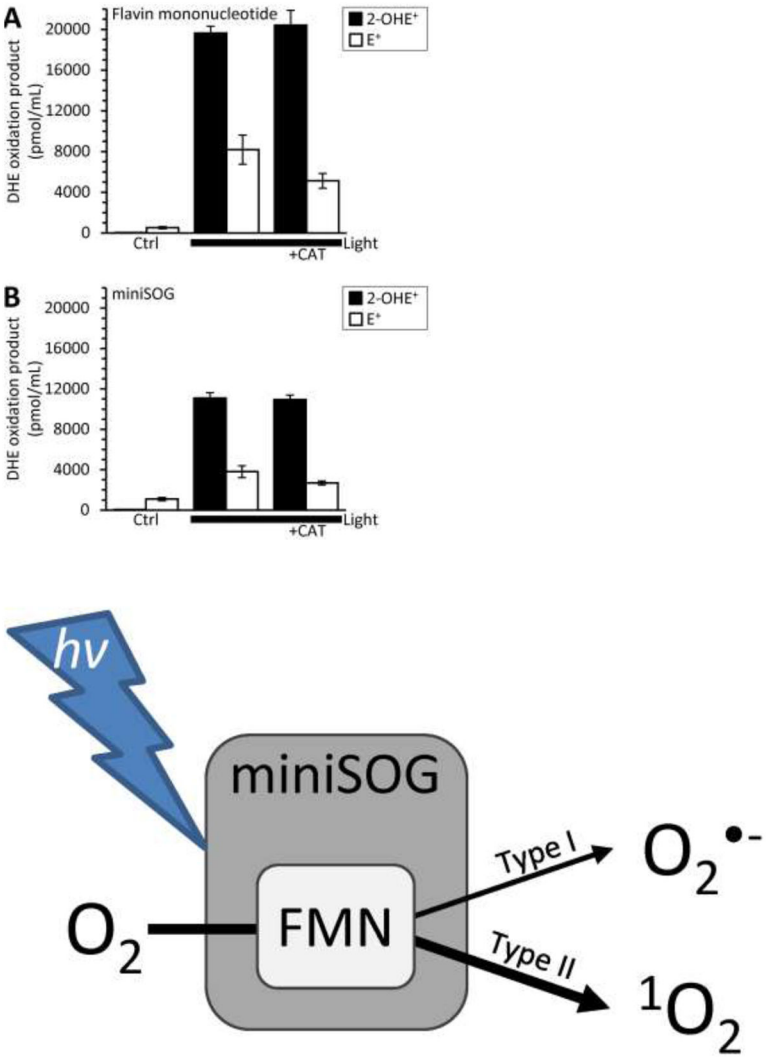

Fig. 5.

H_2O_2 scavenger catalase (CAT) does not impact FMN or miniSOG generated $O_2^{\cdot-}$. (A) Free FMN (10 μM) or (B) purified miniSOG (10 μM) were illuminated (470 ± 20 nm; 5.9 mW/mm^2) for 5 minutes in the presence of DHE (50 μM) and CAT (1 mg/mL). DHE illuminated for 5 minutes (no photosensitizer) resulted in 73 ± 37 pmol/mL 2-OHE^+ and 642 ± 37 pmol/mL E^+. CAT had no significant effect on either the 2-OHE^+ or E^+ component (2-way ANOVA with Tukey correction). All data are means ± SEM, N > 4.

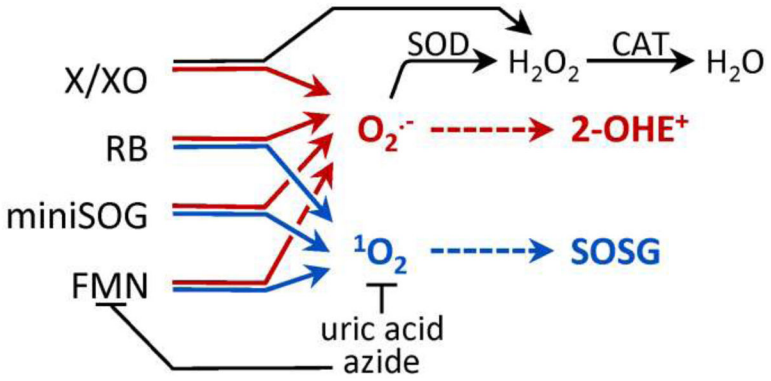

Scheme 1. Overview of ROS detection methods

ROS generators were used to produce superoxide ($O_2^{\bullet-}$) and/or singlet oxygen ($^1O_2$). 2-hydroxyethidum (2-OHE$^+$) is a $O_2^{\bullet-}$-selective marker, while $^1O_2$ was detected using Singlet Oxygen Sensor Green (SOSG). Superoxide dismutase (SOD) converts $O_2^{\bullet-}$ to hydrogen peroxide (H_2O_2), which can be removed by catalase (CAT) to water. Both uric acid and azide quench $^1O_2$, while azide additionally quenches the triplet state of FMN. Abbreviations: X (Xanthine), XO (Xanthine oxidase), RB (Rose Bengal), FMN (flavin mononucleotide).